Threshold stress estimation in Hydrogen Induced Cracking by Small Punch Tests based on the application of the incremental step loading technique

B. Arroyo[*,1], L. Andrea[1], F. Gutiérrez-Solana[1], J.A. Álvarez[1], P. González[1]

[1]LADICIM, Depto. de Ing. del Terreno y de los Materiales, University of Cantabria
Avda. de los Castros, 44, 39005 Santander, Cantabria, Spain
[*]arroyob@unican.es

Abstract

The small punch test consists on punching a plane small specimen until it breaks. This technique, born in the 80's, should be considered when evaluating mechanical properties in situations where materials are in shortage. In recent works, it has been used to estimate the mechanical properties of steels in aggressive environments, where characterizations usually consist on the determination of the threshold stress to avoid subcritical cracking by means of constant loading tests, which is a slow technique, and sometimes presents a considerable dispersion in the results. The standard ASTM F1624 solves these problems, by applying constant loads gradually increased, called loading steps, until the sample fails.

In the present work, it is proposed to apply the incremental step loading technique from ASTM F1624 adapted to the Small Punch Test (SPT). As a novel approach, modifications on the steps durations for SPT are proposed according with the sample thickness, allowing to obtain the threshold stress in aggressive environments within a few days, by using at least 3 samples. The proposed methodology is applied to a set of two steels, of medium and high-strength, in hydrogen embrittlement environments under three different levels of cathodic polarization in an acid electrolyte. As a reference, cylindrical tensile specimens were subjected to conventional standard tests in accordance with ASTM F1624.

The correlation between the threshold stresses, obtained according to ASTM F1624, and the threshold loads, obtained by the Small Punch proposal, is presented and analyzed. Finally, from the aforementioned correlation, a threshold stress estimation based just on Small Punch tests is proposed.

Keywords: Small Punch Test, step loading technique, ASTM F1624, Threshold stress, Hydrogen embrittlement.

Nomenclature

EAC	Environmentally Assisted Cracking
SPT	Small Punch Test
CP	Cathodic Polarization
P_{FFS}	Fast Fracture Load (form tensile test in air ASTM E8)
P_{max}	Maximum load of the first step sequence ASTM F1624
P_{th}	Threshold load ASTM F1624 (final test in environment)
σ_{th}	Threshold stress ASTM F1624 (obtained from P_{th})
P_y	Elastic-to-plastic load in SPT test in air

P_{max}	Maximum load in SPT test in air
$P_{FFS\text{-}SPT}$	SPT Fast Fracture Load (form test in air according to European Standard draft)
$P_{max\text{-}SPT}$	SPT Maximum load of the first step sequence (SPT proposal)
$P_{th\text{-}SPT}$	SPT threshold load (final test in environment SPT proposal)
$\sigma_{th\text{-}SPT}$	Threshold stress estimated by SPT (obtained by proposed correlation)
h_0	SPT sample thickness

1. Introduction

In the last decades, materials have been pushed to the limit, developing a wide range of medium and high-strength steels to satisfy the demands. The disadvantage of these materials, widely used in industrial and high-energy facilities, is that are severely affected by the adverse environments commonly present is these activities. The effect of the environment in these type of steels when operating in offshore marine environments combined with cathodic protection systems or those typical of H_2S presence as in gas transport pipelines, results in Environmental Assisted Cracking (EAC) phenomena, which can lead to the degradation of the steel and to catastrophic failures.

For the above reasons, it is necessary to control medium and high-strength steels that work in harsh environments; some of the two main standards used for EAC characterization are ISO 7539 [1] and ASTM E1681 [2]. Therefore slow strain rate tests are the most commonly employed ones to obtain fracture properties, while tests under constant load are currently used for the threshold stress determination. The threshold stress has historically been defined as the upper limit where failure will never occur, for its determination cylindrical specimens are subjected to constant load up to failure, defining the threshold as the lower loading condition that will cause a delayed fracture when the sample is exposed to a specific environment after a certain time.

This methodology has two main disadvantages: the demand of a big amount of time, as it usually requires around 12 samples that can reach up to 10000h [2] of testing, and its inaccuracy. In order to solve this problem, the standard ASTM F1624 [3] was published. It consists of applying incremented constant load steps, one by one, during determined times, until the specimen's failure takes place, due to the material-environment interaction. This faster method allows to estimate threshold stress in EAC, σ_{th}, of steels harder than 33 HRC within days, by testing a minimum of 3 samples.

In some cases, as for welded joints or shells, samples of sufficient size or thickness cannot be obtained to meet the requirements of the aforementioned standards: the Small Punch Test (SPT), standing out among others, was developed in order to solve this problem. It was firstly applied in 1980s, and is becoming a global alternative to standard testing; its European standard, currently in draft, will be soon released [4]. In the past few years, SPT has proved its effectiveness in characterizing medium and high strength steels in aggressive environments [5-9], so based on this, the implementation of ASTM F1624 step loading technique for SPT testing is proposed, once its viability was proved [10]. In the present work, an experimental characterization for the threshold stress is estimated based just on Small Punch tests, derived from its application on two steels, medium and a high-strength, in a hydrogen embrittlement environment generated by cathodic polarization (CP) in an acid electrolyte under three different levels of aggressiveness. As a reference, control standard tests on cylindrical tensile specimens in homologous environments are carried out following the ASTM F1624 standard, in order to validate the methodology here in proposed.

2. Background

2.1. Standard ASTM F1624

This testing method measures the load to initiate a subcritical crack growth in steel when exposed to an aggressive environment. It consists on progressively imposing load steps subsequently increased after a certain amount of time (defined in function of the steel) up to the specimen rupture. A schematic explanation can be found in Figure 1, which describes the methodology summarized in the next sequence:

#0: tensile test in air according to ASTM E8 [11] to establish the fast fracture load, P_{FFS}, which will directly be the maximum load for the first step load profile in environment, P_{max}.

#1: first test in environment (step load profile). After pre-charging the sample in the environment, a total of 20 steps (5% of P_{max} each) are subsequently applied up to its failure. The failure load defines the threshold load for the first step.

#2 to #n: the rest of the tests in environment are carried out similarly to #1, but using as the maximum load the threshold form the previous test incremented in 10%. This sequence should be repeated until the difference of the threshold loads of two subsequent tests is less than 5%, defining the threshold load in the environment, P_{th}, as the value obtained in the last test. ASTM F1624 [3] imposes to test at least 3 samples in environment, so even if tests #1 and #2 converge to less than 5%, test #3 should be performed to define P_{th}.

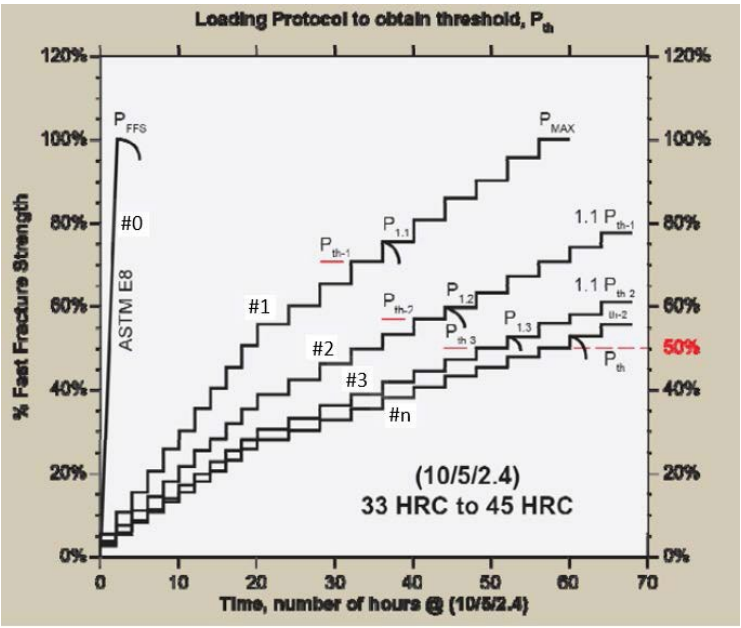

Figure 1 *Example of loading protocol to obtain the Invariant Threshold load, P_{th}, in 33<HRC≤45 steels.*

In general, the higher the tensile properties of the steel, and therefore its hardness, the greater the environmental embrittlement effects on it [12]. Based on this, the standard ASTM F1624 [3] does not include steels with hardness below 33HRC, and defines three different step load profiles in function of the hardness, represented by a numerical code between brackets (see Table

1). This allows to reduce testing times in very hard steels (>54HRC), which usually are high-strength ones, while leaves more time for hydrogen to cause its effects in the softest materials considered by ASTM F1624 (33≤45HRC), which have lower tensile properties and need more time to be affected by hydrogen, accordingly with previous fracture model for EAC induced by hydrogen [13].

Table 1 *Steps load profile depending on the hardness of the steel* [3].

Hardness (HRC)	***Steps***	***Step force ($\%P_{max}$)***	***Step time (h)***	***Steps load profile code***
33 to ≤ 45	*1 to 10* *11 to 20*	*5* *5*	*2* *4*	*(10/5/2.4)*
>45 to 54	*1 to 10* *11 to 20*	*5* *5*	*1* *2*	*(10/5/1.2)*
>54	*1 to 20*	*5*	*1*	*(20/5/1)*

2.2. The Small Punch test

The SPT was firstly documented in 1981 related to the nuclear industry [14], where the limited amount of material for surveillance programs and the difficulty in manipulating large volumes of irradiated steel lead to find alternatives to conventional characterizations. The SPT is a quasi-non-destructive test since the extraction of the small amount of material required does not compromise the component's integrity. As well, testing in-service components can be possible when they have enough material (and allowed to repair sampling hollows). Therefore, SPT has become a worldwide alternative for the estimation of mechanical properties when it is not possible to obtain specimens that fit regular standards. It has been successfully employed in the evaluation of tensile [15] fracture [16] and creep [17] properties of different materials. A European standard, now in final revision draft [4], will be soon published, covering tensile, creep and fracture properties estimations

Because of its reduced dimensions and simplicity, this technique has been applied to characterize embrittlement situations on steels, such as the evolution of materials properties with neutron irradiation [18], the brittle-ductile transition temperature of metallic materials [19], or as above mentioned, in the last decade, environmental embrittlement characterization [5-10].

SPT consists of punching a plane specimen (0.5mm of nominal thickness and less than 1cm^2 of cross section) deforming it until break. Figure 2 shows the device used for the performance of the tests is this work, according the European standard draft [4].

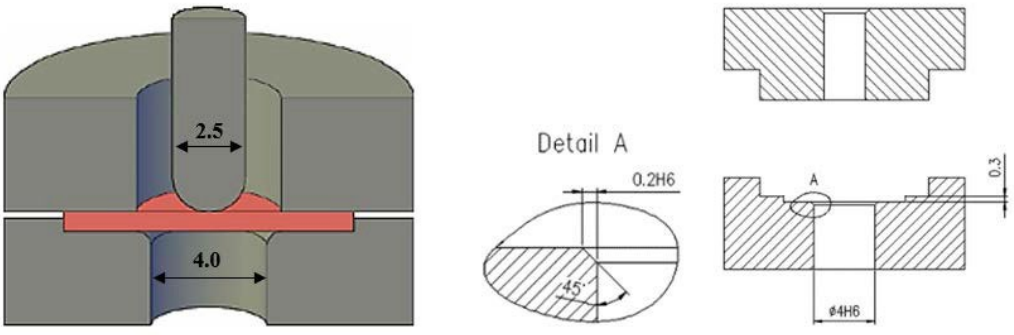

Figure 2 *Small Punch Test experimental device used in this work (left) including the recommendations of the European standard draft* [4]. *Dimensions in mm.*

During the test, the force and the punch displacement are registered continuously, obtaining the type of curves shown in Figure 3 [8]. In ductile scenarios (Figure 3.a) the curve has four zones and two changes of curvature in its initial part, as well as the specimen presents a rupture surface a semicircular shape (smile-type). In brittle or embrittled scenarios (Figure 3.b) the curve has just three zones and one change of curvature, being completely convex after it, being the specimen breaking multi radial (star-type). The different zones of the Small Punch curve represent [8]:

- I: behavior of the sample as an elastic circular plate of embedded in its entire contour and subjected to a centered vertical load.
- II: behavior of the sample as a plastic plate; the first inflexion point from concave to convex, P_y (or P_{I-II}), marks the end of zone I and the beginning of zone II.
- III: behavior of the sample as membrane; the second inflexion pint from convex to concave, P_{II-III}, marks the transition from plate to membrane behavior. Brittle samples do not show membrane behavior, so zone III does not take place and the second convexity change does not take place.
- IV: final instability caused by localized effects at a certain point of the periphery of the sample that leads to the final instabilitly.

In both cases, two main parameters can be pointed:

- P_y: elastic-to-plastic load, marks the beginning of plastics effects on the specimen, ergo the end of its pure elastic behavior; is identified with the first convexity change in the curve.
- P_{max}: maximum load reached during the test, after which the sample's collapse is imminent. The energy below the test curve, E_{SP}, is defined up to this maximum load.

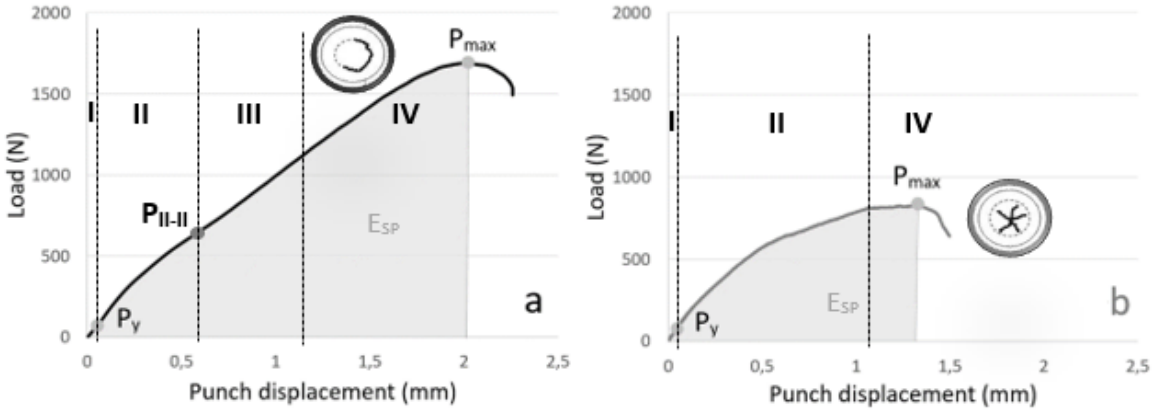

Figure 3 *Schematic of the SPT Load-Displacement curves; a) ductile material, b) brittle material.*

In previous researches [7], it has been proved that the test rate is one of the most relevant variables when SPT is applied to EAC situations, as it happens also in standard environmental characterizations [20]. SPT under constant loads, or at very slow punch rates, are proposed in order to obtain a proper reproduction of EAC micromechanisms taking place in real subcritical processes [7] [8]. Under such conditions hydrogen has enough time to be released from reversible traps and move to the new cracking areas subsequently generated during the test, activated by plastic deformation [13] [21].

In [8], interrupted SPT tests under constant loads were carried out, analyzing the register of the punch displacement vs time (d-t register) obtained together with fractographic aspects; although this methodology is appropriate to obtain threshold loads in environment by SPT tests, it is highly time demanding. For this reason, once recently was proved the viability of the step loading technique application to Small Punch Tests [10], it appeared as an objective to determine the threshold stress as estimated just from the Small Punch tests results, being the goal of the present work.

3. Experimental methodology

3.1. Materials

A high-strength steel and a medium-strength one susceptible of suffering EAC were selected for this work. On the one hand, a rolled X80 steel [22], which is used in petroleum and gas transportation at low temperatures facilities. On the other hand, a weldable thermo-mechanically treated S420 steel [23], which is mainly employed in offshore structures, power plants and pressure vessels.

The chemical composition of both steels is shown in Table 2, and their mechanical properties in Table 3. Their microstructure is presented in Figure 4, having both a ferritic-pearlitic microstructure, with grain sizes ranging between 5-15 μm for X80 and 5-25 μm for S420.

Table 2 *Chemical composition of the two steels analyzed (weight %).*

	C	***Si***	***S***	***P***	***Mn***	***Ni***	***Cr***	***Mo***	***Cu***	***Al***	***V***	***Ti***	***Nb***
X80	*0.07*	*0.18*	*<0.005*	*<0.005*	*1.83*	*0.03*	*-*	*0.15*	*0.02*	*0.03*	*-*	*-*	*0.03*
S420	*0.08*	*0.28*	*0.001*	*0.012*	*1.44*	*0.03*	*0.02*	*0.003*	*0.015*	*0.036*	*0.005*	*0.015*	*0.031*

Table 3 *Mechanical properties of the two steels analyzed.*

	E (GPa)	***σ_y (MPa)***	***σ_u (MPa)***	***e_u (%)***	***HRC***
X80	*209.9*	*621.3*	*692.9*	*29.6*	*33*
S420	*206.4*	*447.7*	*547.1*	*21.7*	*35*

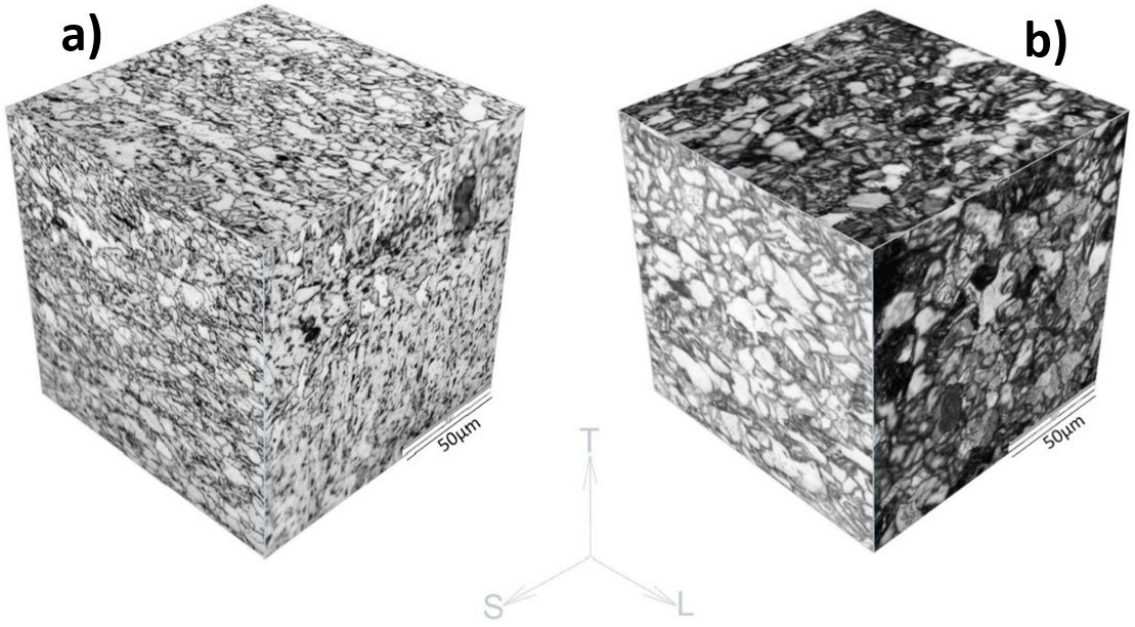

Figure 4 *Microstructure of (a) X80 and (b) S420 steels.*

3.2. Environments selected

The materials selected, when used in oil&gas facilities and off-shore industry environments, will be subjected to the presence of hydrogen, which can damage the material by Hydrogen embrittlement (HE) or by Hydrogen Induced Cracking (HIC) processes [24]. In order to simulate a wide range of the most aggressive HIC situations that can take place in the aforementioned scenarios, cathodic polarization is used to produce hydrogen to be adsorbed and absorbed into the metal samples [25]. Different hydrogen concentration levels are obtained by using different levels of fixed current intensity [26], in order to simulate different aggressively conditions.

The specimen, a platinum grid and the saturated calomel electrode were used as the working electrode, the counter electrode and the reference electrode respectively. Three levels of current density of 1, 5 and 10 mA/cm^2 defined the aggressiveness levels of the environment. The acid electrolyte was consisting of a 1N H_2SO_4 solution in distilled H_2O, containing 10mg of an As2O3 solution and 10 drops of CS2 per liter of dissolution; the As2O3 solution was prepared following the Pressouyre´s method [21]. The pH was measured in the range 0.65-0.80 during the tests and at room temperature (20±2 ºC).

The resulting polarization causes that hydrogen atoms are absorbed on the host lattice [27] increasing the hydrogen concentration, origin of global or local embrittlement mechanisms The aqueous solution was in continuous stirring and/or circulation [1] to remove hydrogen bubbles on the specimen surface, and prevent localized corrosion deposits (e.g., pits) or local environmental conditions. A schematic of the cathodic polarization set-up employed during the tests is shown in Figure 5.

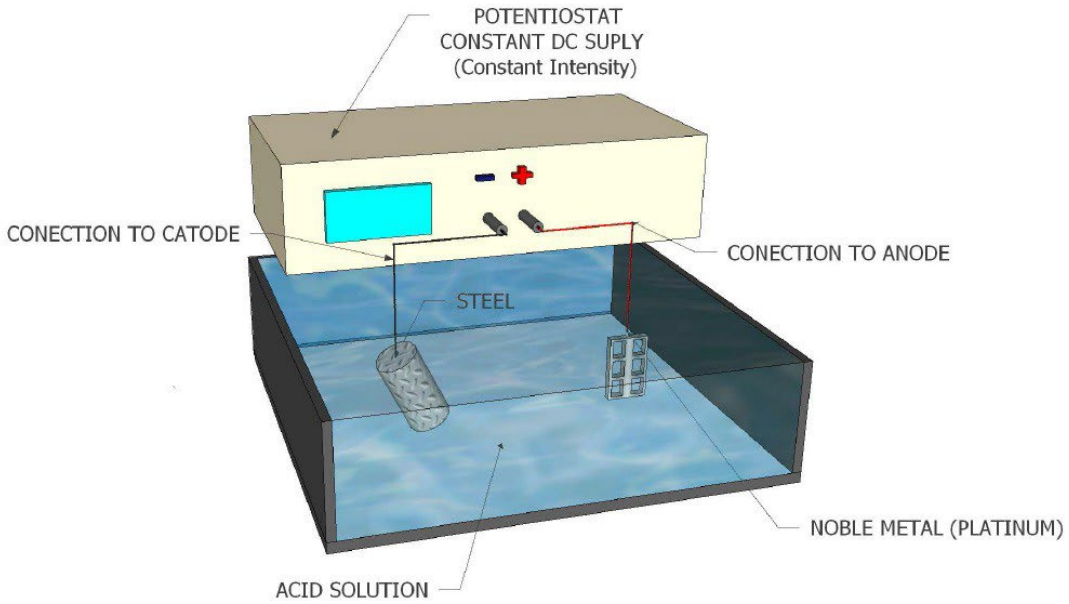

Figure 5 *Schematic of the cathodic polarization set-up employed.*

3.3. Tensile tests according ASTM F1624

For each environment, tests on cylindrical specimens according ASTM F1624 [3] were performed, following the methodology explained in epigraph 2.1. This allowed to obtain the threshold load, P_{th}, and its corresponding threshold stress, σ_{th}, for X80 and S420 steels in the aforementioned three environments. According to [11], two sets of Ø6mm cylindrical specimens were obtained from plates of both steels in TL orientation; dimensions are shown in Figure 6.

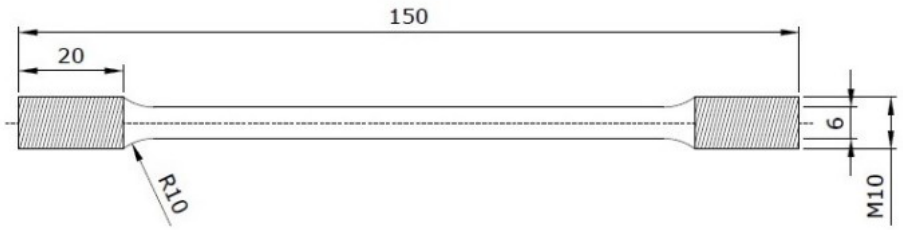

Figure 6 *Schematic of the tensile specimens employed for ASTM F1624 tests.*

As explained in epigraph 2.1, the ASTM F1624 [3] standardized methodology was employed. In the present work, for X80 steel of 33 HRC and S420 of 35 HRC, a (10/5/2.4) step protocol was corresponding in both cases, according to Table 1, ergo 10 steps 2h long and 10 more steps 4h long. Prior to starting each steps sequence, the specimens were subjected to hydrogen absorption by exposing them for 24 hours to the same environment and aggressiveness conditions as the test itself, a time considered sufficient [21] for a proper homogenous hydrogen distribution.

The samples tested in environment, according to the recommendations of [1], were placed in an electrolytic cell specially designed in such a way that the central part was completely immersed inside the aqueous solution during the whole test, while the solution was in continuous re-circulation in the cell; Figure 7 shows a general view of the experimental set-up. In order to achieve a total electrical isolation of the process, the zones of the specimen coincident with the wall passages were coated with an insulating varnish, and then covered by a plastic blushing to avoid local pitting, as shown in Figure 8. Figure 9 shows a detail of the experimental set-up, where hydrogen production in the environment during the test can be observed.

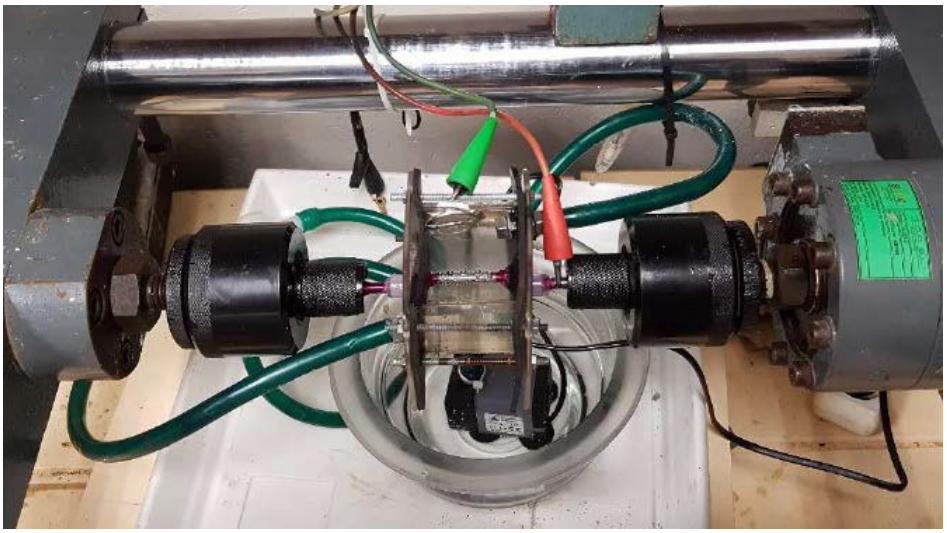

Figure 7 *General view of the experimental set-up for tests according ASTM F1624.*

Figure 8 *Detail of isolation of the zones of the specimens coincident with the wall passages of the electrolytic cell in tests according to ASTM F1624.*

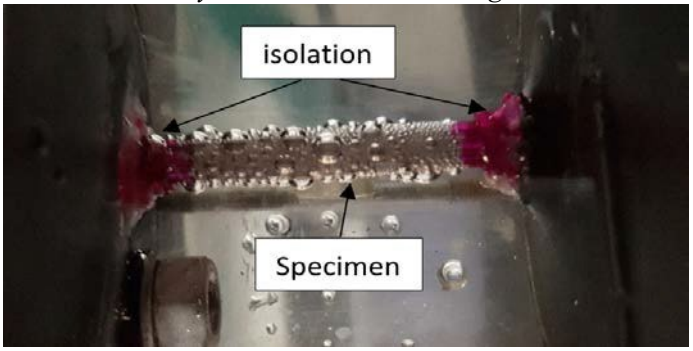

Figure 9 *Detail of hydrogen production in the environment during ASTM F1624 tests.*

3.4. Proposal for Small Punch step loading methodology

To implement the step loading technique methodology from ASTM F1624 [3] to the SPT, its essence, exposed in section 2.1 and applied to the materials and environments studied in this work in section 3.3, is maintained in order to obtain the SPT threshold load, $P_{th\text{-}SPT}$. However, in the present work some new requirements have been made attending to considerations relative to the specimens dimensions and diffusion throw the thickness collected in [8], as well as the own testing procedure:

1. The fast fracture load for SPT tests, $P_{FFS\text{-}SPT}$, was defined as the maximum load, P_{max}, reached during a SPT test in air according to the European SPT standard working draft [4] at 0.01mm/s of punch rate (instead from a tensile test according to ASTM E8 [11]). Also, for further analysis, the elastic-to-plastic load, P_y, was obtained as the first inflexion point of the curve, as previously explained in section 2.2 (see Figure 3); for this purpose a spreadsheet software was employed to adjust a polynomial fit of degree 6 to the initial part of the curve, which first inflection point was then identified.

2. The exposure time of the samples to the environment prior to the steps application was of two hours; this time, which is the result of a study conducted by the authors of the present work, has been previously proposed [8] [9] [10] to pre-embrittle SPT samples in environment prior to mechanical testing. It is more than the strictly necessary if compared to the 24 hours employed for the ϕ6 mm cylindrical samples (see section 3.3), taking into account that the time to reach homogeneous conditions is proportional to the square of the thickness of the specimen.

3. Shorter times for loading steps were considered, proposing, in the present case for steels with a (10/5/2,4) step protocol, 10 steps 20 minutes long and 10 more steps 40 minutes long. These times are again long enough to be sure that the hydrogen diffusion throw the sample thickness was complete, as well as to be operative a complete test in a working day.

A set of SPT specimens was obtained from each one of the two materials studied. The SPT specimens had a thickness of 0.5±0.01mm (taken into account in further analysis, see section 4.5, to minimize its impact and preserve accuracy) and a square cross section of 10x10mm^2, as proposed by several authors [6-10] (equivalent to the Ø8mm currently used and by the European SPT standard draft [4]). The surface was finished employing grain size #2000 water-sanding paper. In Figure 10 a schematic of the specimens employed is presented, which were tested, according to [4] (see Figure 2), with a Ø2.5 mm hemispherical punch head together with a 45º- chamfered jig with a testing process zone of Ø4 mm in all the cases.

As indicated in the European SPT standard draft [4], in order to characterize the materials in L orientation, as it is the case for the tensile specimens used as reference in the present work, SPT samples thickness was orientated perpendicularly to the direction of the axis of tensile specimens, as shown in Figure 10. This means that the cross section of the specimens is contained in the L-T plane, and stresses during punching will be developed in both L and T directions. So, in cases of an important anisotropy between L and T directions, if T direction is the weakest one , it will cause the SPT sample failure, resulting then non-representative direction tensile mechanical behavior and then no comparable to the performed reference tensile test. The aforementioned issue is not present in the steels employed in this work, but this intrinsic limitation of the Small Punch test should be taken into account in case of high anisotropy, in order for not to obtain inaccurate or wrong results when applying the proposed methodology.

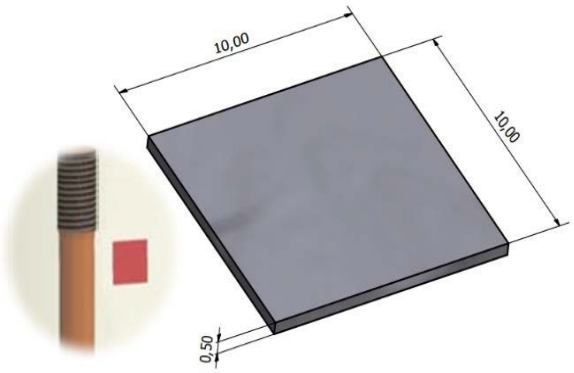

Figure 10 *Schematic of the Small Punch specimens and its orientation compared to tensile specimens. Dimensions in millimeters.*

To carry out these tests, the experimental device shown in Figure 11 was designed and built specifically for this purpose. It basically consists on an electrolytic cell in which the SPT sample is embedded between two rigid jigs and punched by the action of the load. The loading steps are applied by the action of weights on the punch, which can be so softly applied that will avoid any bump or dynamic effect. The sample is completely immersed inside the aqueous solution during the whole test, while the solution is in continuous re-circulation in the cell. In order to achieve a total electrical isolation of the process, the punch was coated with an insulating varnish and its hemispherical head was made of a ceramic material, also the jigs are built in an insulant plastic material.

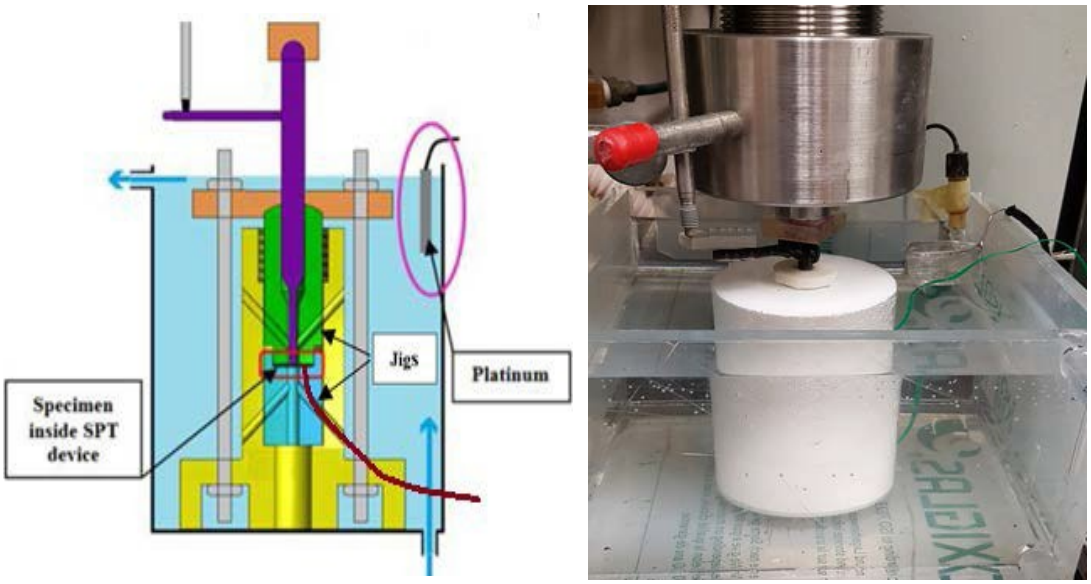

Figure 11 *Schematic (left) and picture while working (right) of the Small Punch device built for performing tests under the step loading technique.*

4. Experimental results and discussion

4.1. Tensile tests according ASTM F1624

Figure 12 shows the step profiles obtained in both materials by using the ASTM F1624 [3] standard as previously described, while Figure 13 presents the fratographies of the sample form the last step profile tested in each case. Finally, Table 4 presents a summary of the numerical results obtained.

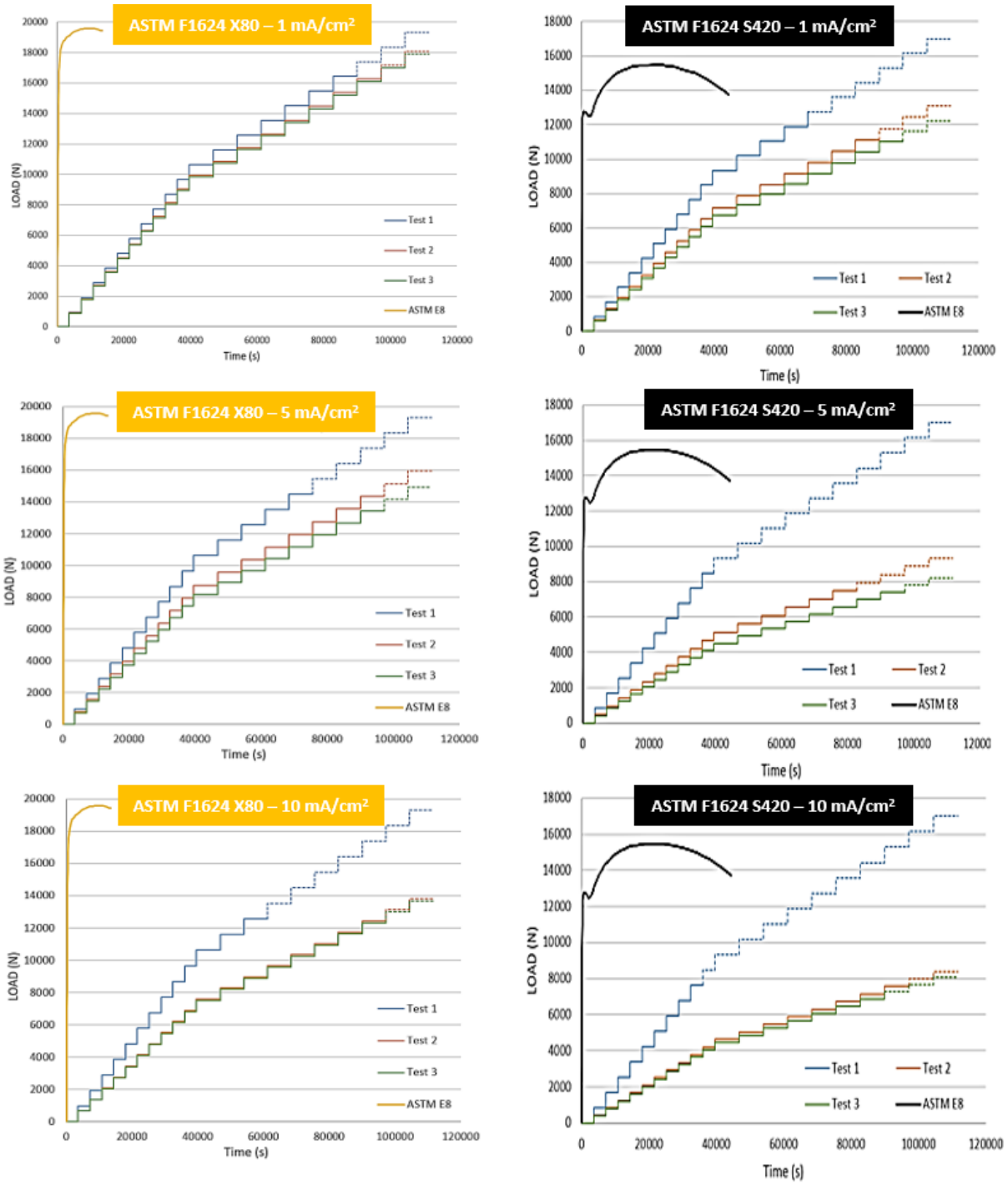

Figure 12 *Stress-time registers of X80 (left side) and S420 (right side) steels obtained by applying ASTM F1624* [3] *when tested in a cathodic polarization environment of 1 mA/cm² (top), 5mA/cm² (center) and 10 mA/cm² (bottom); the dashed lines show the planned steps that did not take place after specimen failure.*

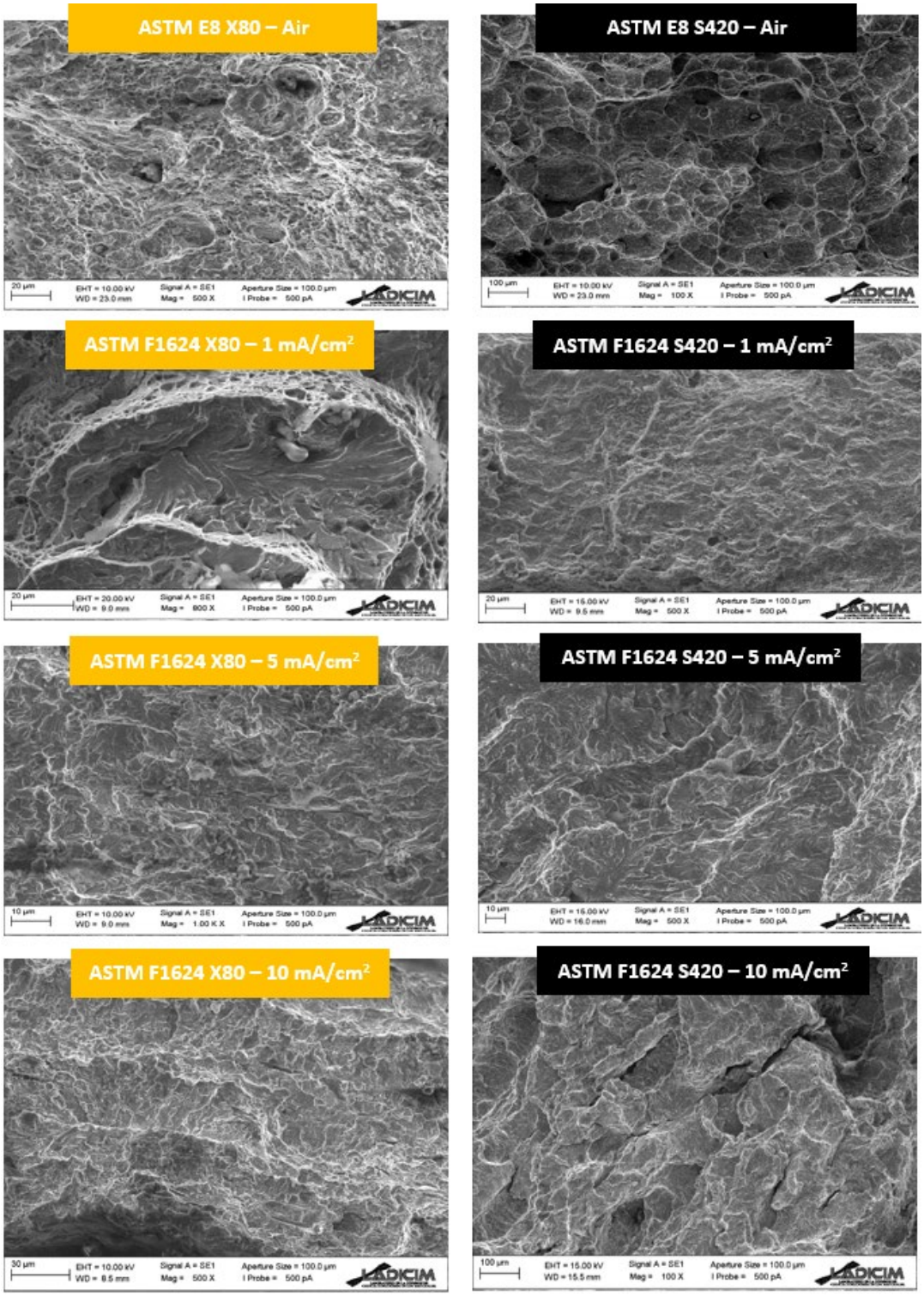

Figure 13 *Fractography of ASTM F1624* [3] *tests on X80 (left side) and S420 (right side) steels in air (top), and under cathodic polarization environments of 1 mA/cm² (center-top), 5mA/cm² (center-bottom) and 10 mA/cm² (bottom); the images shown correspond to the sample form the last step profile tested in each case.*

Table 4 *Numerical results from ASTM F1624* [3] *tests.*

	Air		***1 mA/cm²***	***5 mA/cm²***	***10 mA/cm²***
	S_y (Mpa) *(Table 3)*	***S_u (Mpa)*** *(Table 3)*	***σ_{th} (MPa)***	***σ_{th} (MPa)***	***σ_{th} (MPa)***
X80	*621.3*	*692.9*	*556.10*	*446.46*	*436.01*
S420	*447.7*	*547.1*	*379.47*	*265.29*	*257.98*

4.2. Small Punch step loading tests

Figure 14 shows the step profiles obtained in both materials by using the SPT step loading methodology proposed, as previously described, while Figure 15 presents the fratographies of the sample form the last step profile tested in each case. Finally, Table 5 presents a summary of the numerical results obtained.

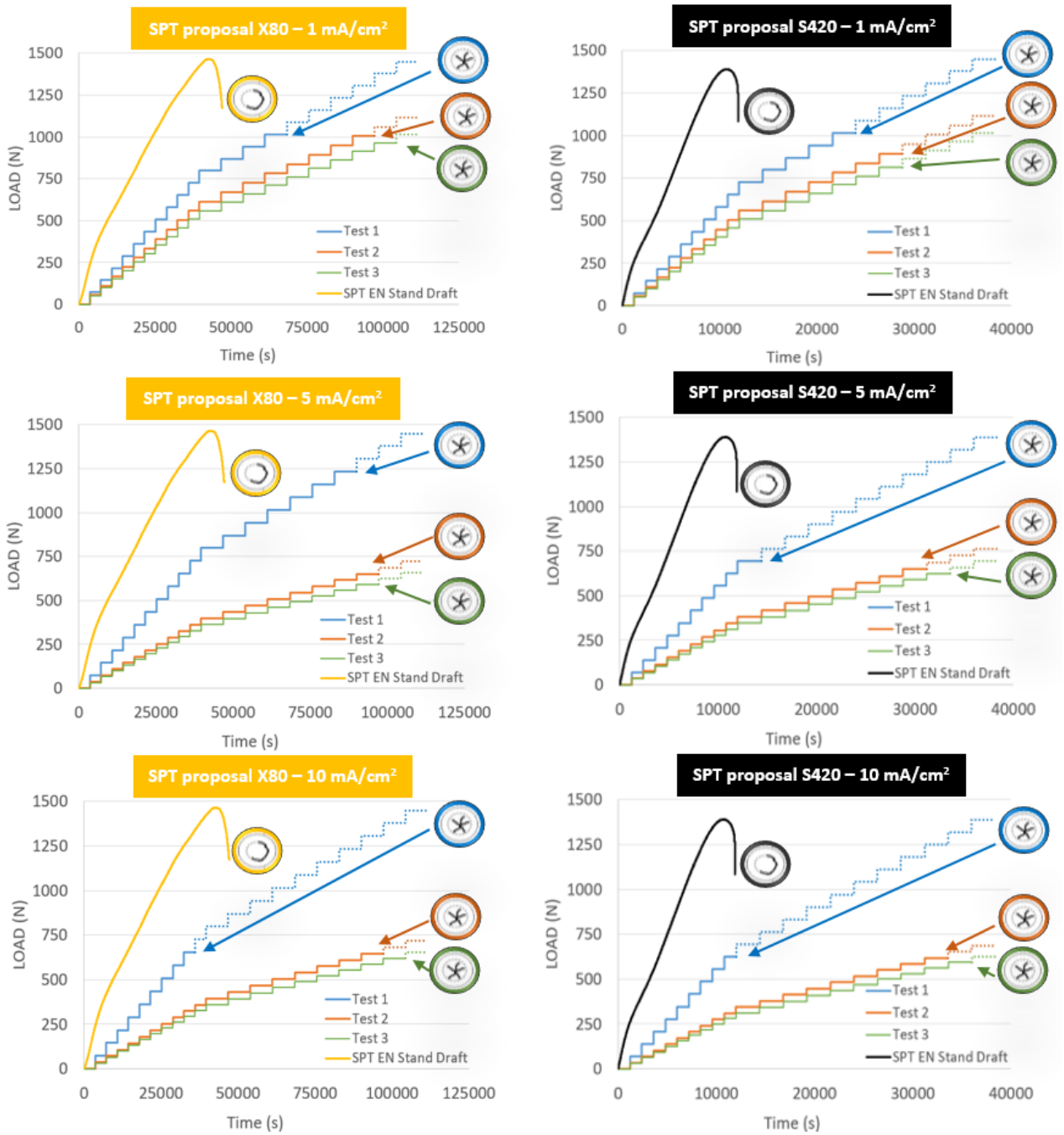

Figure 14 *Load-time registers of X80 (left side) and S420 (right side) steels obtained by applying the SPT loading technique proposal when tested in a cathodic polarization environment of 1 mA/cm² (top), 5mA/cm² (center) and 10 mA/cm² (bottom); the dashed lines show the planned steps that did not take place after specimen failure.*

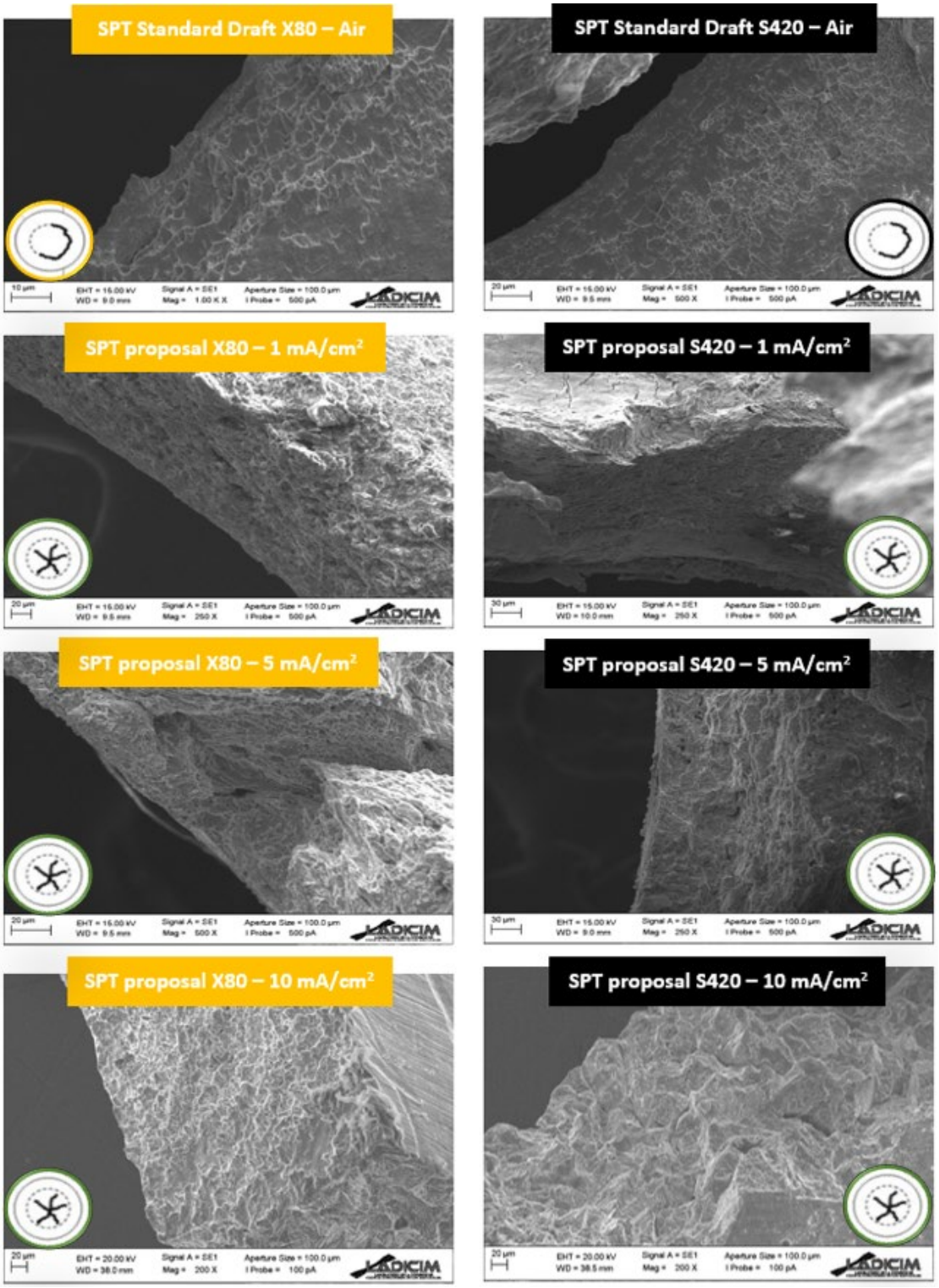

Figure 15 *Fractography of ASTM F1624* [3] *tests on X80 (left side) and S420 (right side) steels in air (top), and under cathodic polarization environments of 1 mA/cm² (center-top), 5mA/cm² (center-bottom) and 10 mA/cm² (bottom); the images shown correspond to the sample form the last step profile tested in each case.*

Table 5 *Numerical results from SPT proposal tests.*

	Air		***1 mA/cm²***	***5 mA/cm²***	***10 mA/cm²***
	P_y (N) *(Figure 3)*	***P_{max} (N)*** *(Figure 3)*	***$P_{th\text{-}SPT}$ (MPa)***	***$P_{th\text{-}SPT}$ (MPa)***	***$P_{th\text{-}SPT}$ (MPa)***
X80	*121*	*1490*	*943*	*638*	*620*
S420	*69*	*1465*	*812*	*625*	*594*

4.3. Comparison between both techniques results

The main goal of the present work is to estimate the threshold stress in aggressive environment applying the incremental step loading technique to the Small Punch test. In order for this to work properly, it is necessary that it has a physical sense, ergo the results from both techniques under the same environmental conditions should be compared to check that behaviors at a macroscopic scale as well as in relation to micro-mechanisms taking place are similar.

Firstly, by regarding Figure 12 and Figure 14, corresponding to ASTM F1624 [3] and SPT proposal step registers, it can be stated that presented similar main characteristics in both techniques. For homologous environments, the number of septs sequences necessary to converge to the threshold (number of samples tested) was the same in all the cases, also the load reduction with respect to the fast fracture load was qualitatively similar. So, it can be stated that the overall appearance of the step sequences was similar in both techniques.

Concerning the micromechanisms taking place, if Figure 13 and Figure 15 are compared a similar conclusion can be stated. On the tests in air from both techniques (ASTM E8 vs SPT standard draft) ductile micromechanisms can be observed for both materials, which are mainly consisting of microvoids. On the tests in environment, it can be seen how both, ASTM F1614 [3] and SPT proposal, are able to show progressive embrittlement effect respecting the tests in air as environment aggressiveness (current density) applied increases. In both materials, the ASTM F1624 tests under 1 mA/cm^2 showed a mixed behavior showing some cleavages (of bigger entity in the case of X80 steel), fact that was also observed in the SPT samples fratographies. When the aggressiveness is increased to 5 mA/cm^2, a clear transgranular mechanism together with more important cleavages took place in ASTM F1624 tests, being also reflected in the SPT proposal samples. Finally, the results at 10 mA/cm^2 were, slightly more brittle, but very close to the ones at 5 mA/cm^2 in both techniques and materials, which showed that the material was very close to its hydrogen saturation at 5 mA/cm^2, and also that the proposed SPT technique was able to show this effect similarly to the standard ASTM F1624 method.

Finally, regarding Table 4 and Table 5, that includes a summary of the numerical results from both techniques, Figure 16 can be built correlating the threshold stresses and forces obtained by ASTM F1624 [3] and SPT proposal respectively. It can be observed how for each of both materials there is an evident linear embrittlement trend among the three environments studied, arriving in both cases to saturate the hydrogen effect, as in 5 and 10 mA/cm^2 environments the thresholds are quasi-equivalent, as mentioned above. Besides the excellent correlation also it can be appreciated that the slopes in both regression lines are almost identical (0.309 for X80 vs 0.327 for S420), establishing a constant proportionality between the reduction in threshold tensile stresses and threshold SPT forces due to embrittlement in both materials, having both the same ferritic-pearlitic microstructure [12].

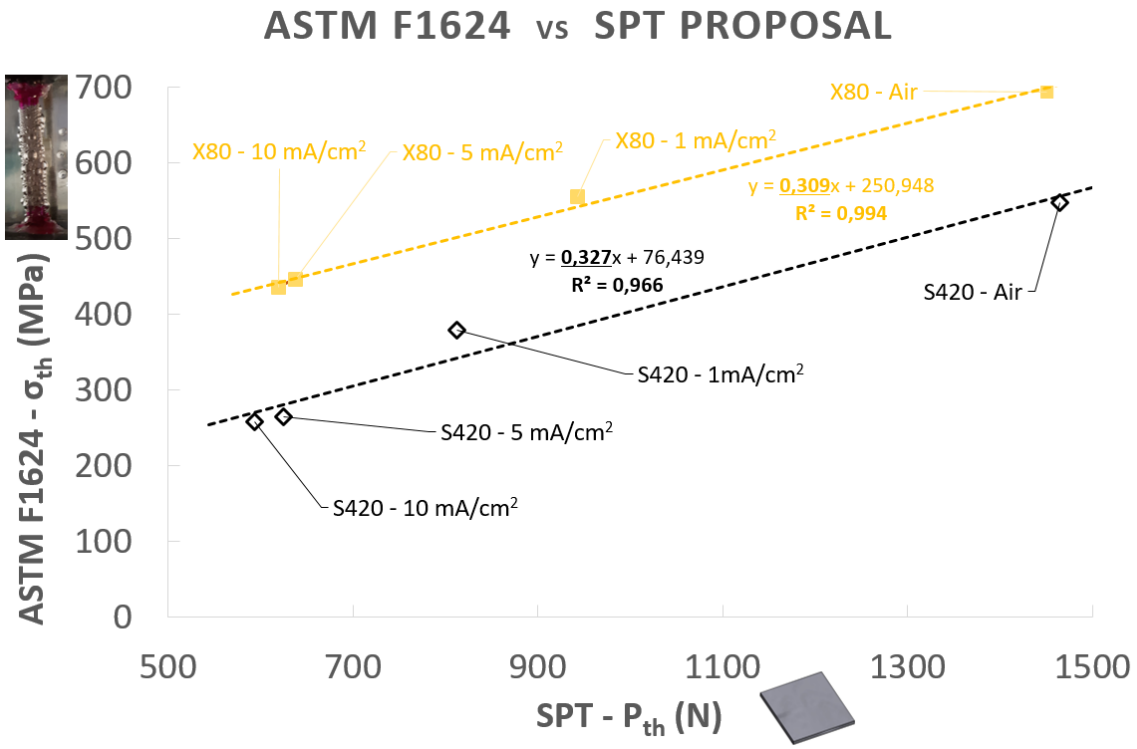

Figure 16 *Results from threshold stresses according ASTM F1624* [3] *vs SPT threshold loads obtained by applying the proposal on X80 and S420 steels in the environments studied.*

4.4 Hydrogen concentration effect into embrittlement

Concerning the observed hydrogen saturation conditions, a very small difference between the 10 mA/cm^2 environment and the 5 mA/cm^2 can be found one in both materials. This takes place in the standard ASTM F1624 [3] tests as well as in the SPT proposed ones, which proves that the SPT is able to reflect the severe hydrogen saturation conditions in the material accurately (as previously displayed on Figure 16).

In order to verify this effect, and the gradual effect of hydrogen concentration, hydrogen content tests on both materials under the environments studied were carried out. For this purpose the hot extraction technique was used, employing the simple acetone cleaning method and following the overall recommendations proposed in [28]; a total of 5 samples was tested for each scenario adopting the mean as a result. The results, presented in Table 6, support the above reasoning, as the contents for 5 and 10 mA/cm^2 environments in both materials were very close one to another (less than 2.5% of difference), being 1 mA/cm^2 one intermediate between air and saturated condition.

Table 6 *Hydrogen content analysis results*

	Air *(as received)* ***(ppm)***	***1 mA/cm^2*** ***(ppm)***	***5 mA/cm^2*** ***(ppm)***	***10 mA/cm^2*** ***(ppm)***
X80	*0.89*	*6.20*	*9.79*	*10.01*
S420	*0.92*	*8.75*	*12.02*	*12.33*

In order to show the hydrogen content effect in the threshold stresses obtained by applying ASTM F1624 (Table 4) as well as in the SPT proposal ones (Table 5), Figure 17 shows its graphical representation (in MPa for ASTM F1624 values and in N for SPT ones) vs the hydrogen content (Table 6). In the vertical axis, the represented values of threshold stress (MPa) or load (N) are calculated as the decrement respecting the value obtained in air, as well as in the horizontal axis the hydrogen content increment is also calculated from the value of both materials in air.

A constant proportionality between the reduction in threshold tensile stresses or threshold SPT forces can be established in function of the hydrogen content increment, which is shown in Figure 17. Similarly, as stated from Figure16, it can be observed how there is a linear embrittlement trend among the four environments studied (including air conditions) for both materials in σ_{th} reduction as well as in P_{th} reduction, indicating an extremely good correlation between hydrogen embrittlement effect, measured by any of the testing procedures, and hydrogen content.

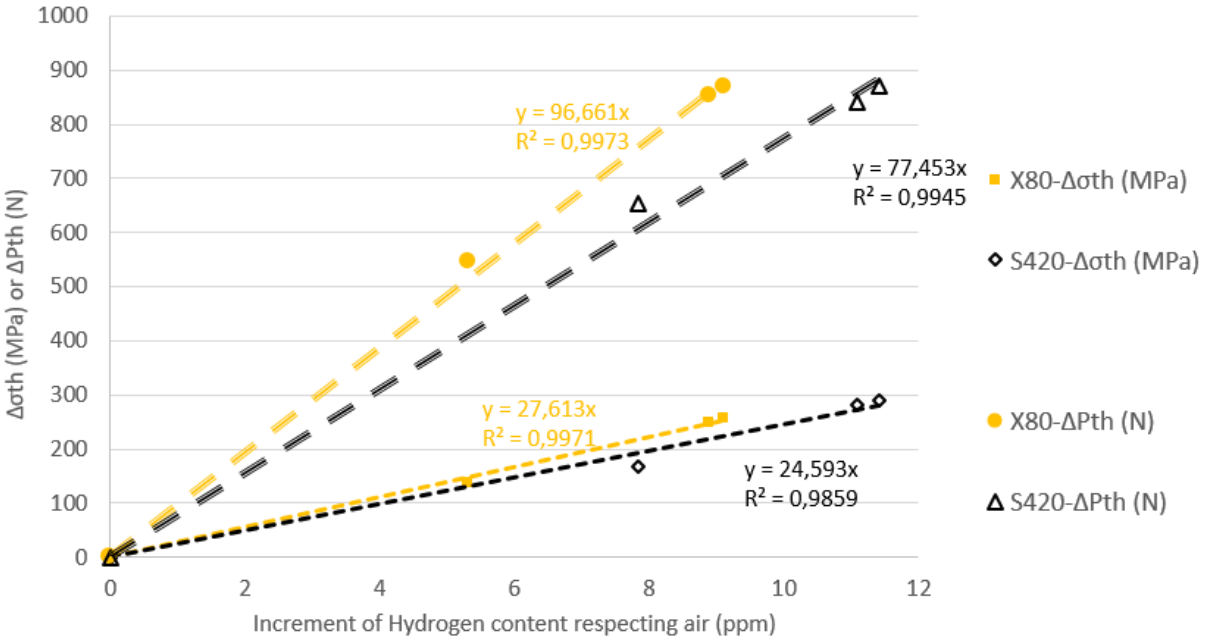

Figure 17 *Reduction in the threshold tensile stresses according ASTM F1624* [3] *(left) and threshold SPT forces from the proposed methodology (right) vs the hydrogen content in the environments studied for X80 and S420 steels.*

4.5 Threshold stress estimation by step loading SPT tests

When the numerical values obtained from the tests carried out in the present work, are studied in detail, it can stated that in Table 5, for the tests according to SPT proposal, the threshold loads obtained, $P_{th\text{-}SPT}$, are in all the cases smaller than the maximum load of the SPT test performed in air, P_{max}, but much higher than the elastic-to-plastic load of the material in air, P_y, ergo:

$$P_y < P_{th\text{-}SPT} < P_{max} \tag{2}$$

Then, as presented in Figure 16, a constant proportionality between the reduction in threshold tensile stresses and threshold SPT forces due to embrittlement in both materials is represented by the aforementioned almost identical slopes in both correlation lines. This phenomena should be then dependent on the plastic component of the load, (P_{th}-P_y).

Accordingly, an expression to estimate the threshold stress, $\sigma_{th\text{-}SPT}$, from an SPT test threshold load, $P_{th\text{-}SPT}$, by adding an elastic component, σ_{el}, and a plastic one, σ_{pl}, can be proposed:

$$\sigma_{th-SPT} = \sigma_{el-SPT} + \sigma_{pl-SPT} \tag{3}$$

Where $\sigma_{el\text{-}SPT}$ is the elastic component, which will be determined from the elastic-to-plastic load of the SPT test, P_y, that marks the beginning of the plastic phenomena, and is described in section 2.2 (Figure 3). According to the elastic theory of plates [29] the maximum stress on the lower surface of a circular plate of thickness "h_0" embedded in its entire contour and subjected to a centered vertical load in the center of the plate, "P_y", responds to the expression:

$$\sigma_{el-SPT} = \frac{3}{2 \cdot \pi \cdot {h_0}^2} \cdot P_y \tag{4}$$

And σ_{pl} is the plastic component, that can be obtained according to numerous approaches in literature to estimate stresses from SPT loads [4] [30] [31], which are all based on the load of the

SPT test, in this case "($P_{th\text{-}SPT}$ - P_y)", and the thickness of the specimen, "h_0". For this case the following structure, which implies a dimensionless correlation coefficient, "α" is proposed:

$$\sigma_{pl-SPT} = \frac{\alpha}{{h_0}^2} \cdot (P_{th-SPT} - P_y) \quad (5)$$

From this, entering "P_y" and "$P_{th\text{-}SPT}$" in N and "h_0" in mm, expression (6) is proposed for the best fit ($\alpha = 0.0806$ and $R^2 = 0.960$). The results obtained from its application are presented in Figure 18, where it can be observed that the results are inside the ±10% error interval, which is accepted as the general uncertainty in fracture mechanics, mainly in local fracture mechanics as the subcritical processes observed.

$$\sigma_{th-SPT} = \sigma_{el-SPT} + \sigma_{pl-SPT} = \frac{3}{2 \cdot \pi \cdot {h_0}^2} \cdot P_y + \frac{0.0806}{{h_0}^2} \cdot (P_{th-SPT} - P_y) \quad (6)$$

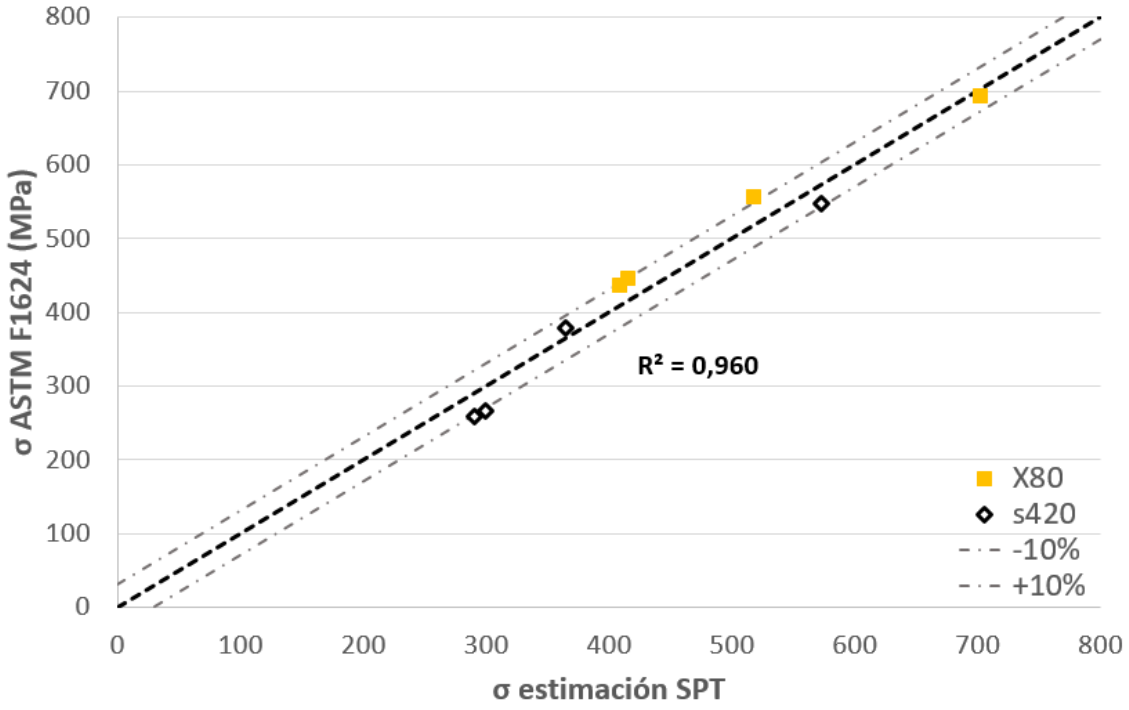

Figure 18 *Best fit for threshold stress obtained by the application of the expression (7).*

Looking back to Figure 16, slopes from both materials (m=0.309 for X80 and m=0.327 for S420 can be expressed as follows:

$$\Delta\sigma_{th-SPT} = m \cdot \Delta P_{th-SPT} \quad (7)$$

On the other hand, the increment of threshold stress, from expression (6), can be written as:

$$\Delta\sigma_{th-SPT} = \sigma_{th-SPT} - \sigma_{el-SPT} = \sigma_{pl-SPT} = \frac{0.0806}{{h_0}^2} \cdot (P_{th-SPT} - P_y) = \frac{0.0806}{{h_0}^2} \cdot \Delta P_{th-SPT} \quad (8)$$

Identifying expressions (7) and (8) and introducing the mean thickness of the samples employed in this work, h_0=0.501 mm, a mean value for the slope m = 0.321 when considering both materials is obtained.

$$m = \frac{0.0806}{{h_0}^2} = \frac{0.0806}{0.5^2} = 0.321 \quad (9)$$

This value is between the slopes for X80 and S420 obtained in Figure 16, and very close to their mean (0.318); the slight difference corresponds to the fact that in the experimental correlation from Figure 18 the dimensionless parameter α=0.0806 was calculated by a regression of the values introducing the exact sample thickness from each test (from 0.49 to 0.51mm), while in expression (9) the mean thickness of 0.501 mm (very close to the nominal 0.5 mm) was employed.

5 Conclusions and future work

In the present work, a technique to estimate the threshold stress by SPT means in aggressive environments, that was conceptualized by the authors in a previous work [10] and is based on the incremental step loading technique form ASTM F1624 [3], has been validated, presenting a new experimental correlation which allows to obtain a threshold load, $P_{th\text{-}SPT}$, within days by using at least 3 specimens.

To adapt the aforementioned methodology to small punch testing, the fast fracture load for SPT tests, $P_{FFS\text{-}SPT}$, has been defined as the maximum load in a SPT test in air, P_{max}, according to the European SPT standard working draft [4] at 0.01mm/s of punch rate; for further analysis, the elastic-to-plastic load, P_y, is obtained. It has also been proposed to expose the samples during two hours to the environment prior to the steps application, as stated in literature [8-10] for 0.5 mm specimens. And finally, it has been proposed to apply 10 loading steps of 20 minutes and 10 more steps of 40 minutes, considering the hardness of the steels used (33 and 35 HRC), which are long enough to be sure that the hydrogen diffusion throw the sample thickness was complete as well as to be operative to perform test in a working day; this steps times can be optimized.

The same trends in terms of steps profiles development were observed in both cases. Also, SEM studies showed up similar progressive embrittlement effects due to hydrogen presence on subcritical cracking processes in both SPT and standardized ASTM F1624 [3] tests for homologous environments.

An evident linear embrittlement trend among the three environments studied was observed for each one of the materials studied, showing excellent correlations with almost identical slopes, establishing a constant proportionality between the reduction in threshold tensile stresses and threshold SPT forces due to embrittlement in both materials.

SPT tests were able to reproduce the embrittlement effect of hydrogen accurately, up to the saturation conditions. Also a constant proportionality between the reduction in threshold tensile stresses (calculated from ASTM F1624) and threshold SPT loads (calculated from SPT proposal) could be established in function of the hydrogen content.

Finally, an expression was proposed to estimate the threshold stress by SPT means, $\sigma_{th\text{-}SPT}$, from the threshold load obtained by the aforementioned SPT step loading methodology, P_{th}. It involves an elastic part derived form the elastic-to-plastic load from an SPT test in air, P_y, and a plastic part obtained from ($P_{th\text{-}SPT}$ - P_y).

$$\sigma_{th-SPT} = \sigma_{el-SPT} + \sigma_{pl-SPT} = \frac{3}{2 \cdot \pi \cdot {h_0}^2} \cdot P_y + \frac{0.0806}{{h_0}^2} \cdot (P_{th-SPT} - P_y) \quad (6)$$

As a future work, in order to validate this promising methodology and its indirect determination of threshold conditions, further research that contemplates different microstructures, higher steel grades and other environments will be necessary. An important point to focus on will be its application to other steels having higher hardness properties, in order to cover the entire ranged marked in ASTM F1624; materials in the ranges 45<HRC≤54 and HRC>54 must be validated in the future.

6 Bibliography

[1] ISO 7539, Parts 1 to 9, Corrosion of Metals and Alloys, 2011

[2] ASTM E1681-03, Test Method for Determining Threshold Stress Intensity Factor for Environment Assisted Cracking of Metallic Materials, 2013

[3] ASTM F1624-18, Standard Test Method for Measurement of Hydrogen Embrittlement Threshold in Steel by the Incremental Step Loading Technique, 2018

[4] EN Standard Working Draft WI, Metallic materials- Small punch test method, Documents of ECISS/TC 101, AFNOR, 2018

[5] T. Bai, P. Chen, K. Guan, «Evaluaiton of Stress Corrossion Cracking susceptibility of Stainless Steel 304L with Surface Nanocrystalization by Small Punch Test,» Materials Science & Engineering A, vol. 561, pp. 489-506, 2013

[6] García T.E., Rodríguez C., Belzunce F.J., Peñuelas I., Arroyo B., «Developement of a Methodology to Study the Hydrogen Embrittlement of Steels by Means of the Small Punch Test,» Materials Science & Engineering A, vol. 626, pp. 342-351, 2015

[7] García T.E., Arroyo B., Rodríguez C., Belzunce F.J., Álvarez J.A., «Small Punch Test Methodologies for the Analysis of the Hydrogen Embrittlement of Structural Steels,» Theoretical and Applied Fracture Mechanics, vol. 86, pp. 89-100, 2016

[8] B. Arroyo, J.A. Álvarez, R. Lacalle, C. Uribe, T.E. García, C. Rodríguez, «Analysis of Key Factors of Hydrogen Environmental Assisted Cracking evaluation by small punch test on medium and high strength steels,» Materials Science & Engineering A, vol. 691, pp. 180-194, 2017

[9] Arroyo B., Álvarez J.A., Gutiérrez-Solana F., Sainz J., Lacalle R., «A perspective of the Small Punch Test Application to the Evaluation of Hydrogen Embrittlement in Steels. Effect of the Punch Rate on Fracture Properties, PVP2018-84066,» de ASME 2018 Pressure Vessels and Piping Conference, Prague, Czech Republic, 2018

[10] Arroyo B., González P., Andrea L., Álvarez J.A., Lacalle R., «Application of the Incremental Step Loading Technique to Small Punch Tests in Hydrogen Embrittlement, PVP2019- 93550,» de ASME 2019 Pressure Vessels and Piping Conference, San Antonio, Texas, 2019

[11] ASTM E8 / E8M 16a, «Standard Test Methods for Tension Testing of Metallic Materials,» 2016

[12] González J.J., Gutiérrez-Solana F., Varona J.M., «The effects of microstructure, strength level, and crack propagation mode on stress corrosion cracking behavior of 4135 steel,» Metallurgical and Materials Transactions A, vol.27A, pp. 281-290, February 1996

[13] Gutiérrez-Solana F., Valiente A., González J.J, Varona J.M., «A strain-based fracture model for stress corrosion cracking of low-alloy steels,» Metallurgical and Materials Transactions A, vol.27A, pp. 291-304, February 1996

[14] Manahan M.P., Argon A.S., Harling O.K., «The development of a miniaturized disk bend test for the determination of post irradiation mechanical properties,» Journal of Nuclear Materials, vol. 103 & 104, pp. 1545-1550, 1981

[15] Eskner M., Sandstrom R.Eskner M., Sandstrom R., «Mechanical property using the small punch test,» Journal of Testing and Evaluation, vol. 32, nº 4, pp. 282-289, 1995

[16] Foulds J.R., Jewett C.W., Viswanathan R., «Fracture toughness by Small Punch testing» Journal of Testing and Evaluation, vol. 23, nº 1, pp. 3-10, 1995

[17] F. Dobes, K. Milicka, «Application of creep Small Punch testing in assessment of creep lifetime,» Mateials Sciene & Engineering A, Vols. 1 de 510-511, pp. 440-443, 2009

[18] Finarelly D., Roedig M., Carsughi F., «Small Punch Tests on Austenitic and Martensitic Steels Irradiated in a Spallation Environment with 530 MeV Protons,» Journal of Nuclear Materials , vol. 328, pp. 146-150, 2004

[19] Kim M.C., Oh Y.J., Lee B.S., «Evaluation of ductile-brittle transition temperature before and after neutron irradiation for RPV steels using Small Punch tests,» Nuclear Engineering and Design, vol. 235, pp. 1799-1805, 2005

[20] Álvarez J.A., Gutiérrez-Solana F., González J.J., «The influence of loading rate on hydrogen induced cracking of microalloyed steels,» Fatigue & Fracture of Engineering Materials and Structures, vol. 20, Nº 5, pp. 717-727, 1997

[21] Bernstein I.M., Pressouyre G.M., «Role of traps in the microstructural control of hydrogen embrittlement of steels,» Noyes Publ, Park Ridge, NJ, Pittsburgh, 1988

[22] Specifcation API 5LD, Specification for CRA clad or lined steel pipe, American Petroleum Institute, 2009

[23] BS EN 10225:2009, «Weldable Structural Steels for Fixed Offshore Structures Technical Delivery Conditions,» 2009

[24] Hamilton J.M., «The challenges of deep-water arctic development,» International Journal of Offshore Polar Engineering, nº 21, p. 241–247, 2011

[25] Wei, R.P., «Hydrogen Effects in Metals,» Bernstein and A.W. Thompson, eds., AIME, New York, NY, pp. 677-690, 1981

[26] J.A. Álvarez, F. Gutiérrez-Solana, «An Elastic-Plastic Fracture Mechanics Based Methodology toCharacterize Cracking Behaviour and its Applications to Environmental Assisted Processes,» Nuclear Engineering and Design, vol. 188, pp. 185-202, 1998

[27] J.P. Hirt, «Effects of hydrogen on the properties of iron and steel,» Metallurgical Transactions A, vol. 11, pp. 861-890, 1980

[28] B. Arroyo, L. Andrea, J.A. Álvarez, S. Cicero, R. Lacalle, "Analysis of samples cleaning methods prior to hydrogen content determination in steel," Metals, vol. 10, Issue 6, no. 723, 2020

[29] Timoshenko, S., Woinowsky-Krieger, S., «Theory of Plates and Shells,», 1950

[30] Mao, X., Takahashi, H., «Development of a Further-Miniaturized Specimen of 3 mm Diameter for TEM Disk (3 mm) Small Punch Tests,» Journal of Nuclear Materials vol. 150, pp. 42-52, 1987

[31] Cheon, J.S., Kim, I.S., «Evaluation of Thermal Aging Embrittlement in CF8 Duplex Stainless Steel by Small Punch Test,» Journal of Nuclear Materials vol. 278, pp. 96-103, 2000